

Gas/Solid Reactions with Acetone

Gerd Kaupp*, Uwe Pogodda, and Jens Schmeyers

University of Oldenburg, Organische Chemie I,
Postfach 2503, D-26111 Oldenburg, Germany

Received May 3, 1994

Key Words: Gas/solid reactions / Imbibition / Acetone derivatives / Atomic force microscopy / Anisotropic phase rebuilding / Waste prevention

Gas/solid reactions of acetone vapor with neutral organic compounds, salts, or host crystals with strict exclusion of solvents are reported. This gas/solid technique largely avoids waste formation and saves resources. Starting hydrochlorides or hydrobromides are also synthesized by gas/solid techniques. Dihydrohalides of *o*-phenylenediamines give 1,5-benzodiazepines **3**, aromatic and aliphatic 1,2-aminothiols (*o*-aminothiophenol, penicillamines, cysteine) yield five-membered thiazolines and thiazolidines **7**, **9**, **11**, **13**. Virtually all carbonyl reagents of the primary amino type **14** give quantitatively the imino derivatives **15** and water. Salt formation may be helpful for increasing melting points and sometimes reactivity as in **8**, **10**, and **12** if surface passivation has to be overcome. In the case of solid **14** the free bases react equally well. Acetone (**2**) may be quantitatively removed from exhaust gases by using hydroxylaminium phosphate with for-

mation of free acetone oxime at high flow rates. Inclusion of acetone into various hosts (**17–20**, but not **16**) is more efficient by imbibition from the gas phase than by crystallization from acetone as the solvent. This advantage may be utilized for gas separations. Some further gases (vapors) coexist in imbibed clathrates whereas others do not. The mechanisms of the gas/solid reactions are elucidated using atomic force microscopy (AFM). Phase rebuildings involve anisotropic movements of molecules over large distances and the formation of characteristic features. In some cases surface hydrates catalyze the gas/solid reaction. Solid-state mechanisms for imbibition from the gas phase into host crystals with formation of clathrates are similar in nature to those of the covalent reactions. These results are correlated with known X-ray crystal structures where available.

Reactions of solids with gases can be run on a preparative scale^[1]. It has been shown by atomic force microscopy (AFM), that distinct long-range transports occur upon gas/solid reactions (without intervening liquids) and that the mechanisms can be classified with respect to the features observed^[2]. There are different features created on different crystallographic faces of the same crystal, and the type of features formed can be correlated with the bulk crystal structure^[3]. Therefore, the new concept of *phase rebuilding* has been devised for non-topotactic solid-state reactions^[3,4]. Thus, for solid-state reactivity it is essential, that the molecules may find a way to wriggle themselves out of the lattice on chemical reaction. They can do so according to eight basic phase-rebuilding mechanisms^[3,4] which permit efficient gas/solid reactions. Therefore, it was of interest to use gas/solid techniques for syntheses, while avoiding waste formation. Clearly, there is a need to improve the most usual acid- or base-catalyzed reactions of carbonyl compounds which produce large amounts of dangerous wastes, when performed in solution.

In this paper we report on ecologically worthy reactions of acetone vapor with crystalline reagents to give crystalline products without any solvent and in the absence of deliquescence without any intervening liquid phase. These reactions proceed better than in solution and largely avoid waste formation.

A) Acetone Gas and 1,2-Diamines or 1-Amino-2-thiols

Solid *o*-phenylenediamines **1** can be converted most easily into their bis(hydrochlorides)-(hydrobromides) by applying gaseous hydrogen chloride (bromide) to them with initial cooling^[1]. These are highly reactive solid powders which may be handled in air when prepared by this technique. In solution monohydrohalides of deliquescing nature are formed^[5]. The dihydrohalides react with acetone gas (**2**) at room temperature to give the dihydrohalides of the 1,5-benzodiazepines **3** quantitatively by consumption of 2 equiv. of **2** and loss of 2 equiv. of water (Table 1). While the salts of **3** are stable compounds, **3** can be liberated by treatment with aqueous sodium hydroxide^[6]. The reactions of

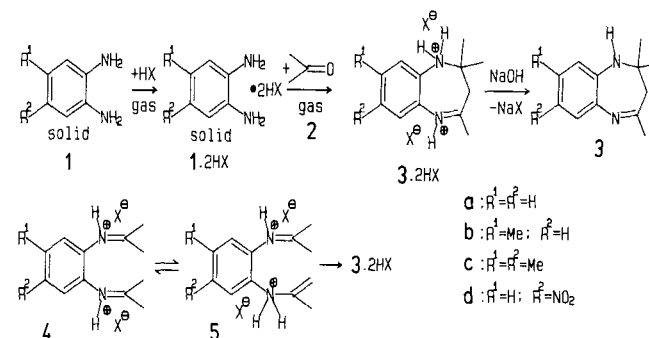


Table 1. Reaction of acetone vapor with solid *o*-phenylenediamine salts **1** · 2 HX, 2-aminothiophenol (**6**), penicillamine salts **8/10**, and cysteine hydrochloride (**12**) at room temperature

Starting solid	M.p. (decomp.) [°C]	Acetone (equiv.)	Time [h]	Product	M.p. (decomp.) [°C]	Yield (%)	Free base	M.p. [°C]
1a · 2 HCl	205	2.0	18	3a · 2 HCl	150	100	3a	125
1a · 2 HBr	260	2.4	12	3a · 2 HBr	90	100	3a	125
1b · 2 HCl	243	2.5	16	3b · 2 HCl	130	100		
1c · 2 HCl	240	2.1	16	3c · 2 HCl	250	100	3c	93
1d · 2 HCl	239	2.0	18	3d · HCl ^[a]	225	71 ^[a]	3d	136
1d · 2 HCl	239	solvent		4d · HCl	185	40		
6	19	1.0	2	7		100	7	45
<i>D</i> - 8 · HCl	196	4.0	16	<i>D</i> - 9 · HCl	196	100	<i>D</i> - 9	198
<i>rac</i> - 10 · HCl	177	4.0	16	<i>rac</i> - 11 · HCl	202	100	<i>rac</i> - 11	172
<i>L</i> - 12 · HCl	175	4.0	16	<i>L</i> - 13 · HCl	169	100	<i>L</i> - 13	138
<i>L</i> - 8 · HCl · H ₂ O ¹²⁷	175	4.0	16	<i>L</i> - 9 · HCl	196	100	<i>L</i> - 9	198

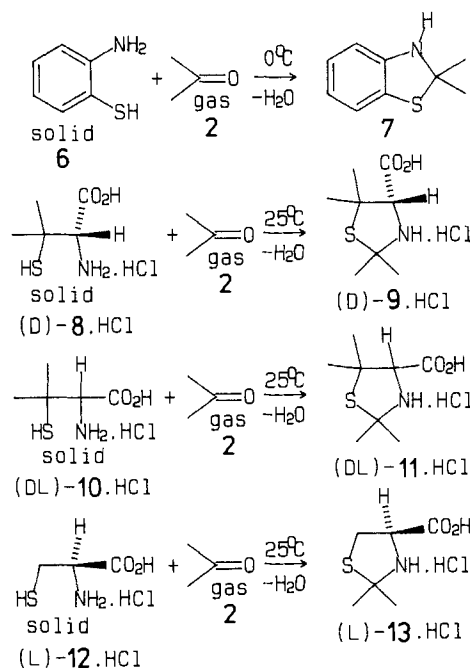
^[a] The raw material contained 20.4% HCl (theory 23.8%); the monohydrochloride (13.5% HCl) was obtained by crystallization from methanol.

1a/d · 2 HX have been run on a 20-g scale, and may be scaled up further.

Interestingly, the above reactions are efficiently acid-catalyzed in the solid state by the monobasic acids HBr and HCl. However, the bis(dihydrosulfate) of **1a** is unreactive. It has to be assumed that in this case there will be no suitable phase-rebuilding mechanism available to the system. Chemically, it must be assumed that initially formed bis(imine) **4** cyclizes by tautomerization to give **5**. This reasonable assumption rationalizes the orientation selectivity of the cyclization. The reaction of **1a** in benzene with mesityl oxide yields **3a** in 28% yield^[7a]. However, it appears unreasonable to assume initial formation of mesityl oxide under our gas/solid conditions. At any rate we did not find any of the possible acetone condensation products in our experiments. The cyclization of the nitro compound **4d** does not occur if the dihydrochloride of **1d** is dissolved in hot acetone and left for crystallization for some days. Only **4d** is isolated from solution. This again points to the superiority of the gas/solid techniques in organic syntheses.

o-Aminothiophenol (**6**) is even more reactive than **1**. Upon application of acetone gas to crystalline **6** at 0°C, the benzothiazoline **7**^[8] and water are formed. Not surprisingly, a five-membered heterocycle is formed here in opposition to the behavior of **1**. However, it will be difficult to decide which of the functional groups is attacked first by **2** in the gas/solid reaction.

The failure of very pure crystalline *D*-(-)-[or (*S*)-]penicillamine (**8**) or *rac*-penicillamine (**10**) and also *L*-cysteine (**12**) to react with **2** might appear puzzling because the nucleophilicities of their functional groups should be higher than those of the aromatic compound **6**. On the other hand, the crystalline hydrochlorides *D*-**8** · HCl, *L*-**8** · HCl · H₂O, *DL*-**10** · HCl, and *L*-**12** · HCl do react to give the versatile thiazolidine salts *D*-**9** · HCl, *L*-**9** · HCl, *DL*-**11** · HCl, and *L*-**13** · HCl in quantitative yield. The hydrochlorides of **9**, **11**, and **13** are not (partially) hydrated as judged from titrations and TGA measurements. The sluggishness of *DL*-**10** to undergo a reaction may be explained with the aid of AFM measurements. They show that after an initial start of the reaction there occurs efficient passivation. Thus, for Figure 1a we



have chosen a section of the (100) surface of *DL*-**10** where there is some roughness (average roughness $R_a = 3.5$ nm). That means, that on the nanometer scale all pertinent crystallographic faces are present here. This is a necessary final test, because on a very flat section on (100) of *rac*-**10** there is no change at all upon application of acetone gas. Only the rough (100) surface gives a reaction producing features with heights of up to 100 nm ($R_a = 11.0$ nm) (Figure 1b). However, these decline upon continuation of the reaction ($R_a = 6.8$ nm) and end with a thin solid cover ($R_a = 1.9$ nm) which protects the crystal (Figures 1c, d). None of these features can be seen or guessed under a microscope at 400 fold magnification. The slight surface reaction which is seen in Figure 1 occurs at crystal faces which are not characterized as (100). The nonreactivity of (100) can be rationalized by molecular packing on the basis of the X-ray data^[9]. In Figure 2 it is seen that on (100) the ammonium and thiol groups of the zwitterion are efficiently shielded

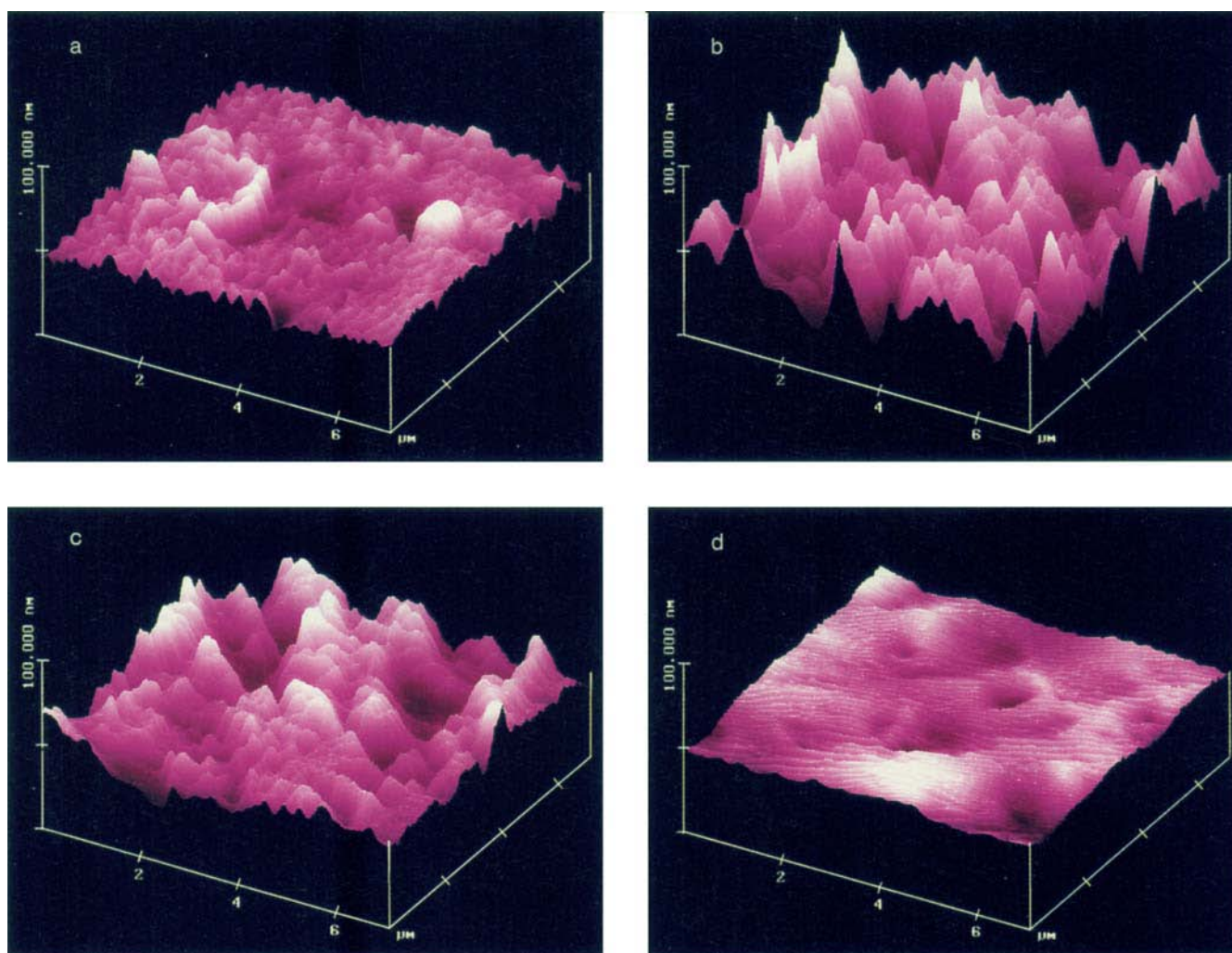


Figure 1. AFM surfaces of the dominant face (100) of DL-10 (from hot water/methanol) at an area of some roughness; a: before; b: after 5 min; c: after 10 min; d: after 30 min exposure to acetone vapor

by the methyl groups which stick out of the surface. Steric hindrance can still be overcome with an island mechanism^[3] if the reaction starts at some molecular defects. However, the efficient passivation by a thin cover as shown in Figure 1 precludes any reaction of DL-10 crystals with acetone (2). This result clearly points out, that solid-state features are more decisive than common chemical reactivity properties.

In contrast to the free amino acids **8**, **10**, **12** their hydrochlorides do react rapidly. As there are no crystal structures available for these, the studies have been extended to the monohydrate $L\text{-}8 \cdot \text{HCl} \cdot \text{H}_2\text{O}$ which reacts equally well in the solid state to give $L\text{-}9 \cdot \text{HCl}$. Figure 3 shows the molecular packing^[9] on the morphologically dominant face. The thiol groups are accessible now on the dominant surface and apparently the HCl prevents any buildup of passivating covers. Thus, the gas/solid reaction may proceed to completion in this and in related salts.

The heterocycles **3**, **7**, **9**, **11**, and **13** are most easily obtained by gas/solid techniques and may be scaled up further. Importantly, waste is largely avoided in these quantitative

procedures. Thus, any waste inherent in solution reactions will be unnecessary from now on. For large-scale productions it will be more practical to remove the heat of reaction on formation of the dihalides $1 \cdot 2 \text{HX}$ with inert gases in a flow reactor as has been described for a similar system on the kg scale^[10] rather than in vacuo.

The orientation selectivities in **3b** and **3d** are interesting. The structures of these products have been consistently derived from their ¹H-NMR spectra which have been analyzed by the additivity rule of the contributions of the various substituents to the chemical shifts. This may be substantiated further by identification of the signal of the isolated aromatic proton without neighboring hydrogen atom.

B) Acetone Gas and Solid Primary Amines

There is a great number of primary amine reagents **14** which form well-defined imines by reaction with carbonyl compounds (Scheme 1). Those products have sharp melting points which serve to characterize the carbonyl compounds, and they are versatile starting materials for the synthesis of

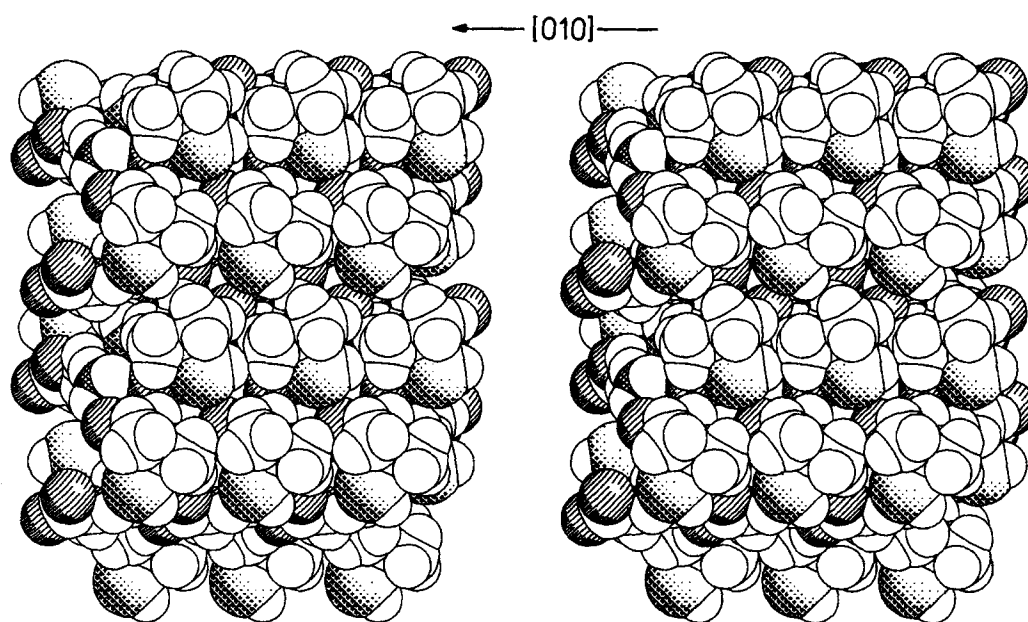


Figure 2. Stereoscopic view of the molecular packing of DL-10 ($P2_1/c$) on (100); N (hardly seen) with grid, S with dots, O with lines

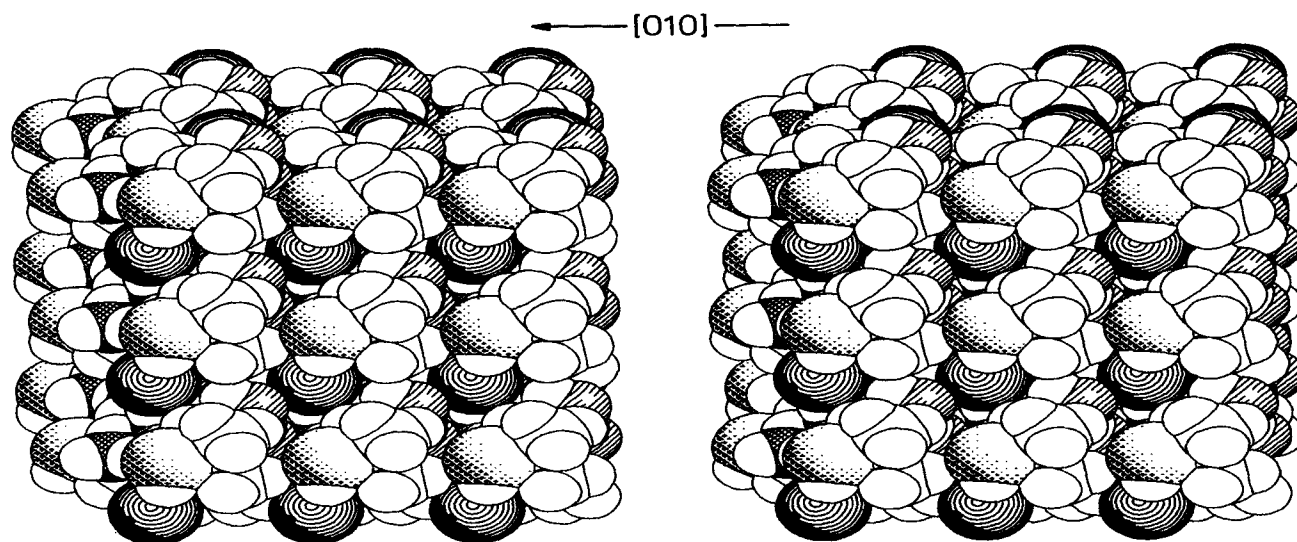
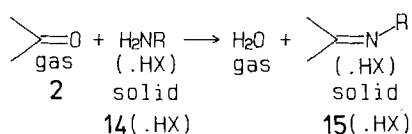


Figure 3. Stereoscopic view of the molecular packing of L-8 · HCl · H₂O ($P2_1$) (from 2 N HCl/H₂O) on (100); N with grid, S with dots, O with lines, Cl with circles

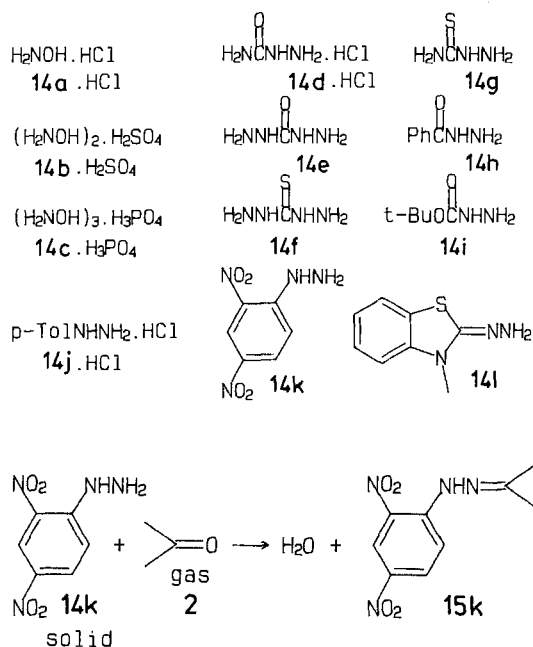
N-heterocycles and rearranged products. These syntheses of carbonyl derivatives are reversible and in most cases catalyzed by strong mineral acids in organic solvents^[11]. Thus, there are formed huge amounts of wastes in solutions. Therefore, it is of the highest interest, that such waste can be avoided by running the reactions of volatile aldehydes and ketones quantitatively as gas/solid reactions.

Scheme 1



We concentrate here on the reactions of acetone (**2**). Gas/solid derivatizations of cyclopentanone and cyclohexanone have been published elsewhere^[12,13]. Usually, **14** is used in the form of its salts. However, if the melting points of the free bases **14** are high enough, these may be directly used for the gas/solid reaction. The bases or salts **14a–l** have been successfully used for quantitative reactions with **2** according to Scheme 1, simply in evacuated flasks. In most cases reactions are complete after ca. 12 h at room temperature. However, the reactions of **14i** and **14f** take 2 and 3d under these modest conditions. All of the products are known in the literature^[11]. They are formed as salts or in free form, depending on the starting material, and characterized spectroscopically and analytically. The oxime salt

15a is hygroscopic and deliquescent (see Experimental). The wealth of the new technique is particularly striking in the case of the uncatalyzed quantitative conversion of 2,4-dinitrophenylhydrazine (**14k**) into its hydrazone **15k**. In ethanol solution this transformation requires concentrated H_2SO_4 or H_3PO_4 as a catalyst and rather tedious workup and waste disposal. In solid-state chemistry this transformation is straightforward rapid, and proceeds quantitatively. Compound **14k** is liberated from most of its adhering water, which is present for safety reasons on shipping and storage of this reagent, prior to the reaction.



For the higher melting reagents **14**(·HX) the reaction rates can be increased by modestly raising the temperatures. This result is important, if the flow technique is chosen for larger scale syntheses or for capture of acetone (**2**) (and other ketones or aldehydes) from exhaust gases. Those experiments show, that the water which is formed as a second product has a catalytic influence and must not be removed completely under too rigorous conditions of temperature and gas flow. However, water does not form liquid nanophases in these cases. Rather, it is needed for the formation of solid surface hydrates of the amino reagents even if those do not form stoichiometric hydrates. This result is shown by the AFM investigations that follow: Hydroxylammonium chloride (**14a**) and sulfate (**14b**) are known to be compounds which do not form crystalline hydrates. They crystallize in unhydrated form from water^[14]. Their morphologically dominant faces are flat when crystallized from methanol. However, AFM reveals, that in ambient (i.e. moist) air surface hydration occurs. In the case of the sulfate **14b** this minute hydration appears to be hindered. Figure 4a shows that it takes about 40 min in moist air under the AFM until hydration starts somewhere and produces moving reaction fronts which arrive at the surface area under study. From there these fronts advance slowly (Figure 4b: 1 h later; 1 more h later still an area of $9 \mu^2$ is flat in the left

front corner of the image, not shown). After 12 h, the image is stable (Figure 4c; also after 22 h). If this surface is exposed to ambient acetone vapor for 4 min, a complete change of the AFM image ensues. In Figure 4d the vertical scale is increased by a factor of 4! Rather smooth structures are formed with some hills on them. The surface stays measurably solid^[3,4]. There are enormous molecular transports in distinct directions. Without previous surface hydration there occurs no rapid reaction of **14b** with acetone vapor.

A completely different behavior is observed with the chloride **14a**. Instead of a zonal mechanism, surface hydration starts at random and so rapidly that it is hard to obtain an area without previous hydration (Figures 5a, 6a). 5 h later the volcano-like hydrates have grown together (Figure 5b). After 1 d, a stable image is obtained (Figure 5c). The surface hydrate reacts now rapidly (2 min) with acetone vapor to give a solid with more than twice as high features as in Figure 5d. It can be shown again, that the reaction occurs only at the sites of hydration. In Figure 6 a surface area has been chosen on the morphologically dominant face of the chloride **14a** (from methanol) which is virtually free of hydrates in large parts. After application of acetone vapor for 3 min, it is seen that the previous features have grown and that the step has advanced from the middle to the right (this has happened about half way after exposure for 2 min, not shown). However, there has virtually occurred no change in the flat unhydrated region (Figure 6b). The reaction starts at the hydrates and at the steps. Later on, the water of reaction will enhance the reaction of the surface. Again, the stable images prove that there is no liquid on the surface at this stage^[3b]. Although the nature and composition of the surface hydrates have not been elucidated so far^[15], the fact that water catalyzes the reactions has to be taken into account for large-scale runs in flow systems with highly diluted acetone (**2**).

C) Large-Scale Formation of Acetone Oxime by Gas/Solid Techniques

The necessity of hydration (in the absence of stoichiometric crystalline hydrates) and the deliquescence of the oxime hydrochloride **15a** make it virtually unfeasible to keep this product solid, if a stream of moist air, which has bubbled through 16.8 g (0.29 mol) of **2**, passes through a column of 20 g (0.29 mol) of **14a** downward at a rate of 460 ml min^{-1} with external heating to 100°C . 80% of the acetone (**2**) are consumed, most of the material has liquefied and is collected in a receiver under the column. The deliquesced hydrochloride **15a** contains water and is not perfectly free of **14a**. However, this experiment proves a high solid-state reactivity.

The sulfate **14b** is less reactive, the reason being the more sluggish surface hydration (Figure 1). Therefore, in a flow system an additional catalyst is necessary. This has been found with KHSO_4 . Thus, in a 1:1 load of **14b** and KHSO_4 under reaction conditions as above, 60–80% conversion of the acetone is achieved in one passage. KHSO_4 prevents sintering/softening. Thus, after several passages or with ex-

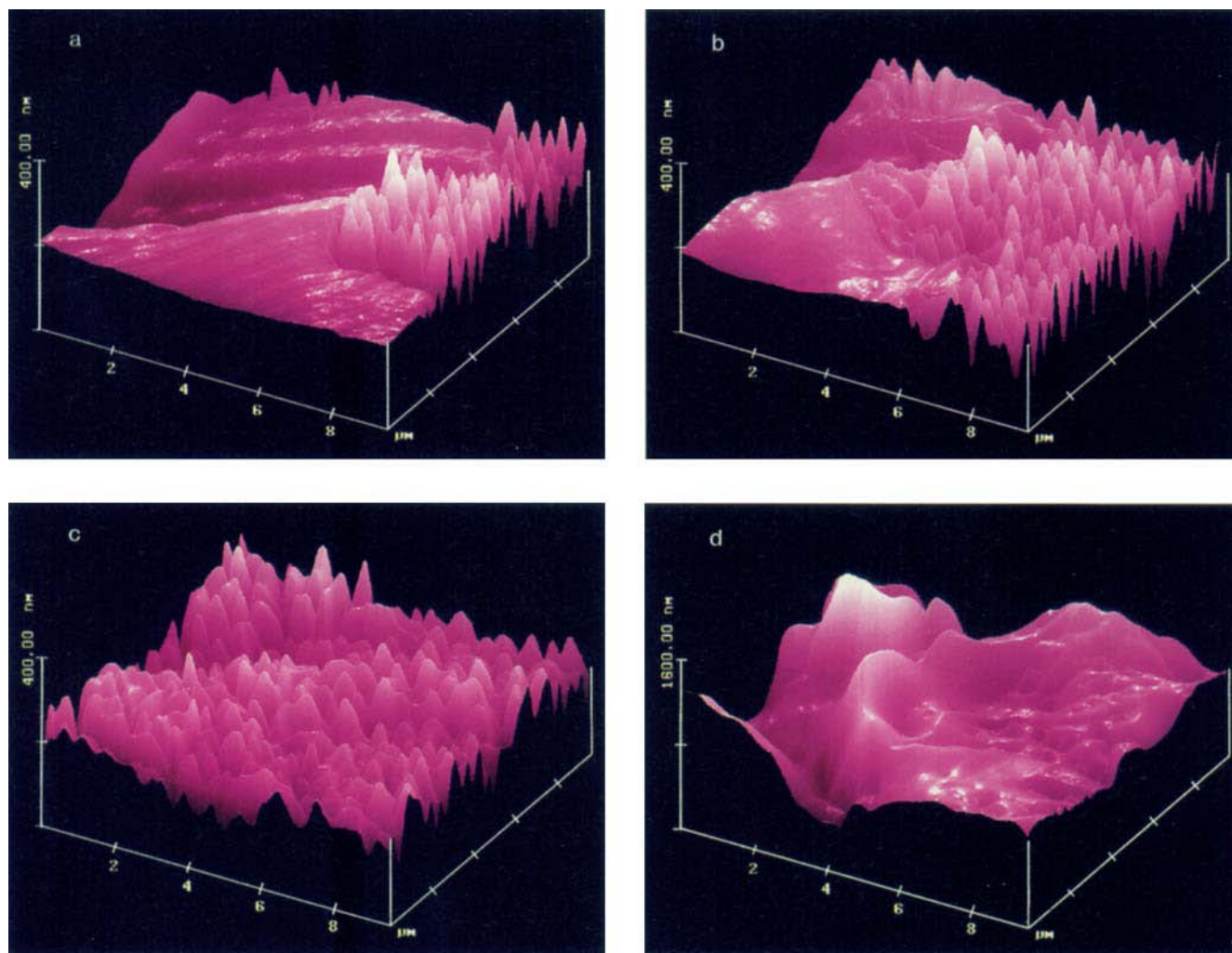


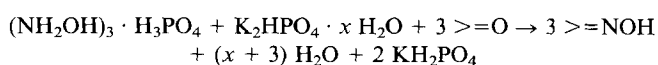
Figure 4. AFM surfaces of the dominant face of the sulfate **14b** (from methanol): a: after 40 min, b: after 100 min, c: after 12 h in moist air at 18°C; d: after reaction of stable surface c (10 more h) with acetone vapor for 4 min

cess **2** solid oxime sulfate **15b** is generated quantitatively though as a mixture with KHSO_4 .

As the gas/solid reactions of acetone (**2**) with primary amino reagents do not necessarily require acid catalysis, a system has been found which keeps sufficient water for surface hydration and liberates acetone oxime but not hydroxylamine from their salts. This approach has the advantage that pure acetone oxime and water will be expelled by the gas stream and easily condensed in a trap at 0°C (or below). Scheme 2 gives the stoichiometry of this gas/solid reaction system. DSC/TGA measurements show that the whole process is thermoneutral (purge gas semisaturated with **2** at 1.4 to 2.1 bar; $\Delta H = \pm 2 \text{ kcal mol}^{-1}$) and that the state of hydration will be as given in Scheme 2 at 80°C. A second reaction here is the stoichiometric solid-state transformation of K_2HPO_4 into KH_2PO_4 . Thus, in a two-column system acetone oxime may be quantitatively formed on a large scale under conditions where all of the acetone (**2**) is allowed to react at high flow rate. Water may be separated from acetone oxime by adsorption on molecular sieves (3-Å type) at 80–100°C or by azeotropic distillation,

preferably with *tert*-butyl methyl ether (TBM). This is the most efficient procedure available for the (larger-scale) synthesis of acetone oxime. Waste can be kept to a minimum, and zero emission in exhaust air is achieved (see Experimental).

Scheme 2



D) Inclusion of Acetone by Imbibition from the Gas Phase

Inclusion reactions lead to supramolecular compounds. The product formations are fully reversible in these cases. Inclusion compounds are well defined and differ in this respect from surface adsorbates. While acetone (**2**) is a suitable guest for various host lattices, its possible inclusion from the gas phase has only recently been achieved^[13,16a], and there are indeed hosts that do not include **2** from the gas phase. Thus, deoxycholic acid (**16**) includes 0.58 equiv. of **2** by crystallization from the latter as a solvent^[16b]. However, if solid dehydrated deoxycholic acid is exposed to ace-

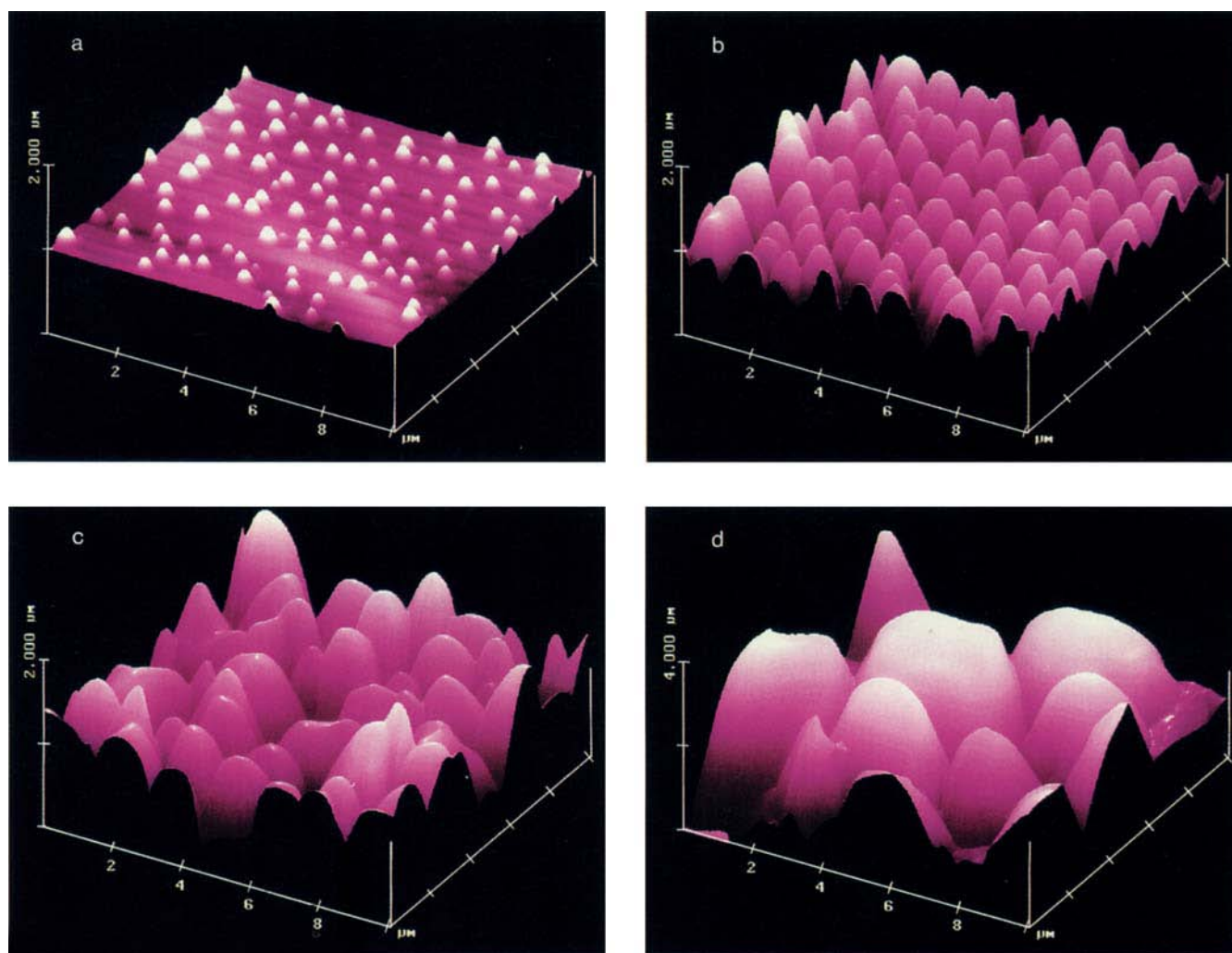


Figure 5. AFM surfaces of the dominant face of the chloride **14a** (from methanol); a: as early as possible (handling for about 10 min); b: after 5 h, c: after 24 h in moist air at 18°C; d: after reaction of surface c with acetone vapor for 2 min

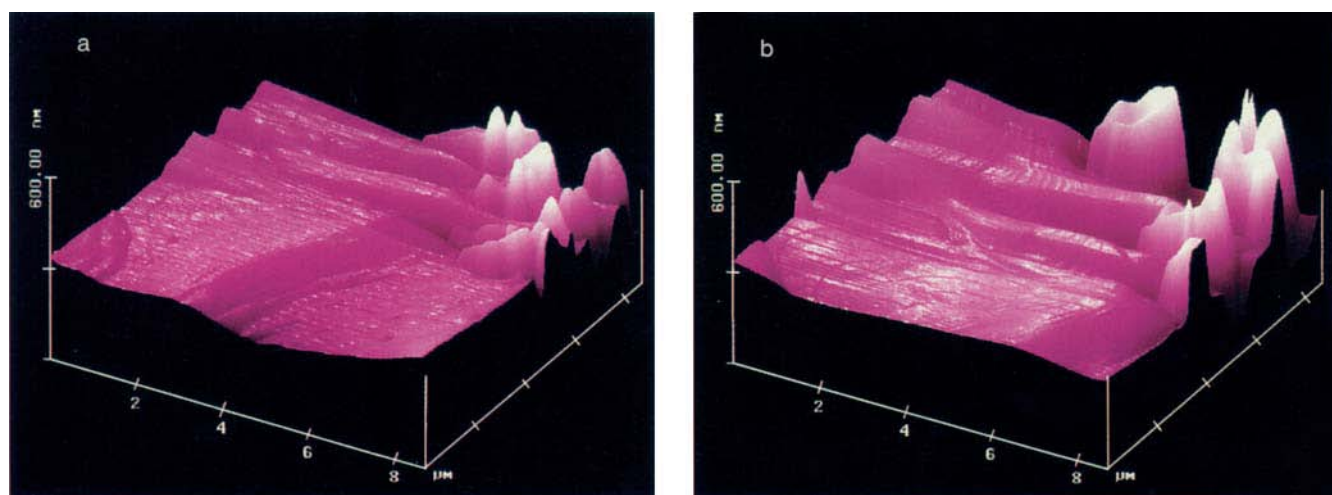


Figure 6. AFM surfaces of the dominant face of the chloride **14a** (from methanol) at an area of only partial hydration; a: as early as possible (handling for about 10 min); b: after reaction of surface a with acetone vapor for 3 min

tone vapor, the latter will *not* be significantly taken up. This result, of course, may not be surprising, because it is well-known, that inclusion compounds do have crystal structures which are different from the pure hosts^[16b,17a]. However, we have been able to find four different hosts (two further hosts in ref.^[16a]) which do imbibe **2** from the gas phase very efficiently. Those inclusion compounds of **17–20** are even more highly loaded with **2** than the counterparts from solution (Table 2).

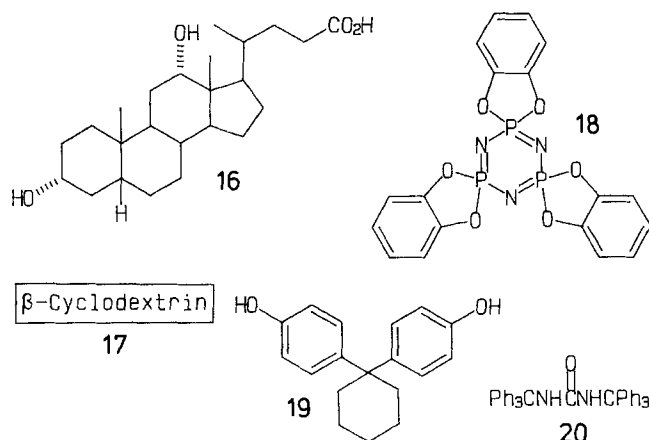


Table 2. Inclusion of acetone (**2**) from the gas phase and by crystallization at room temperature

Host	2 /Host imbibed	$\nu(\text{C}=\text{O})$ [cm^{-1}]	Desorption temperature [$^{\circ}\text{C}$]	2 /Host crystallized
16	—	—	—	0.58 ^[16]
17	2.56	1705	143	1.55 ^[13]
18	0.48 ^[a]	1716	146 ^[a]	0.20
19	0.61 ^[b]	1701	63	0.58 ^[c]
20	0.97	1711	121	0.76

^[a] 0 $^{\circ}\text{C}$; desorption temperature at 10 mbar: 111 $^{\circ}\text{C}$. — ^[b] The value of 12.5 in ref.^[13] is actually the percentage by weight. — ^[c] Dry acetone, desorption temperature 84 $^{\circ}\text{C}$; if commercial acetone with a water content of 0.4% is used for recrystallization only 30 mol-% of **2** are included, desorption temperature 99 $^{\circ}\text{C}$; we could not verify the inclusion of as much as 1 equiv. of **2** by recrystallization (and drying in vacuo) as has been claimed in ref.^[18]. — For **2** in 1,1,6,6-tetraphenyl-2,4-hexadiyne-1,6-diol^[16a] we observed $\nu(\text{C}=\text{O}) = 1702 \text{ cm}^{-1}$ and a sharp desorption temperature of 80 $^{\circ}\text{C}$.

β -Cyclodextrin (**17**) is most efficient. If a stream of ambient air is charged with acetone and passed through a column of solid **17** at room temperature 2.56 equiv. are taken up per host molecule. This process is so efficient, that, up to 85% conversion, there will be no escape of acetone at considerable flow rates. The desorption temperature is 143 $^{\circ}\text{C}$. Interestingly, only 1.55 equiv. of **2** are included by crystallization from solution.

Further solid hosts like **18**^[19], **19**^[20], and **20**^[21] behave similarly in that they imbibe **2** rapidly and more efficiently than by crystallization. Table 2 lists the results and the desorption temperatures in ambient air. From the carbonyl frequencies the extent of polar interaction between guest and host may be judged. It is stronger in **19** than in **17**, **20**,

and **18**. However, desorption temperatures do not correlate, because the carbonyl interaction is only *one* factor which determines the stability. With solid **19** a stream of air (60 ml min⁻¹) loaded with acetone and passed through a column at 0 $^{\circ}\text{C}$ will be completely detoxified until 75% of the saturation of the host material is reached.

It will be important to know if the imbibed and the crystallized clathrates are different in structure. The first hints are provided by their different compositions. Secondly, in the case of **19** where there are particularly sharp onsets in the TGA desorption curves, there are marked differences in the desorption temperatures (63, 84, and 99 $^{\circ}\text{C}$) which depend on the conditions of preparation (Table 2). This finding convincingly points to different structures in this case, even though there are no differences found in the carbonyl frequencies. Unfortunately, imbibition is not a single-crystal-to-single-crystal reaction. Rather, there is disintegration of the crystals which is connected to a decrease in the true density from e.g. 1.59 to 1.35 g cm⁻³ in the case of **18** (1.38 to 1.23 for **20**) and an increase in specific surface from 0.62 to 1.30 m² g⁻¹ for **18** (0.73 to 1.38 for **20**) upon imbibition of **2**. Therefore, no single crystals have been available for an X-ray structure analysis.

It has been shown by Allcock^[17], that the monoclinic form of **18** converts spontaneously to the hexagonal form by exposure of the crystal to the vapor or liquid of certain guest species, including "ketones". As scanning electron microscopy (SEM; after coating with gold)^[17a] only reveals that considerable crystal disruption into fairly uniform microcrystallites (size and morphology) occurs during the transition, we have studied the imbibition mechanism in more detail by using AFM techniques^[2–4]. Guest-free sublimed **18** has a rather irregular natural (001) surface (Figure 7a). It is also seen from the minute edges in Figure 7a, that apparently there has been some prereaction with solvent vapors which happened to be present in the crowded organic chemistry laboratory during manipulation of the crystal (moisture interacts much more slowly within several hours). However, it is perfectly clear from Figure 7b, that upon short exposure to acetone vapor there are formed very pronounced straight edges, which are parallel to the original *b* edges of the lath-shaped crystal (those edges are *not* in scan direction). Thus, it is seen, that during the initial reaction period a new crystalline phase is being formed with molecular movements in very distinct directions in the 100-nm range (Figure 7b). The migration of molecules continues on prolonged exposure (Figure 7c). It can be seen from this image that apparently a secondary phase transformation starts which finally yields the smoother surface of Figure 7d. In this image the ridges are no longer parallel to the *b* axis of the original crystal. No liquid phase is detectable^[3b]. Shortly after proceeding with the acetone application the crystal cracks. Clearly, as in the case of covalent solid-state reactions^[1–4], there is *phase rebuilding* in the supramolecular reaction affording mixed crystals which are rich in starting material. From a certain point of transformation a switch-over to highly enriched product crystals occurs. The composition of the distinct nanostructures in

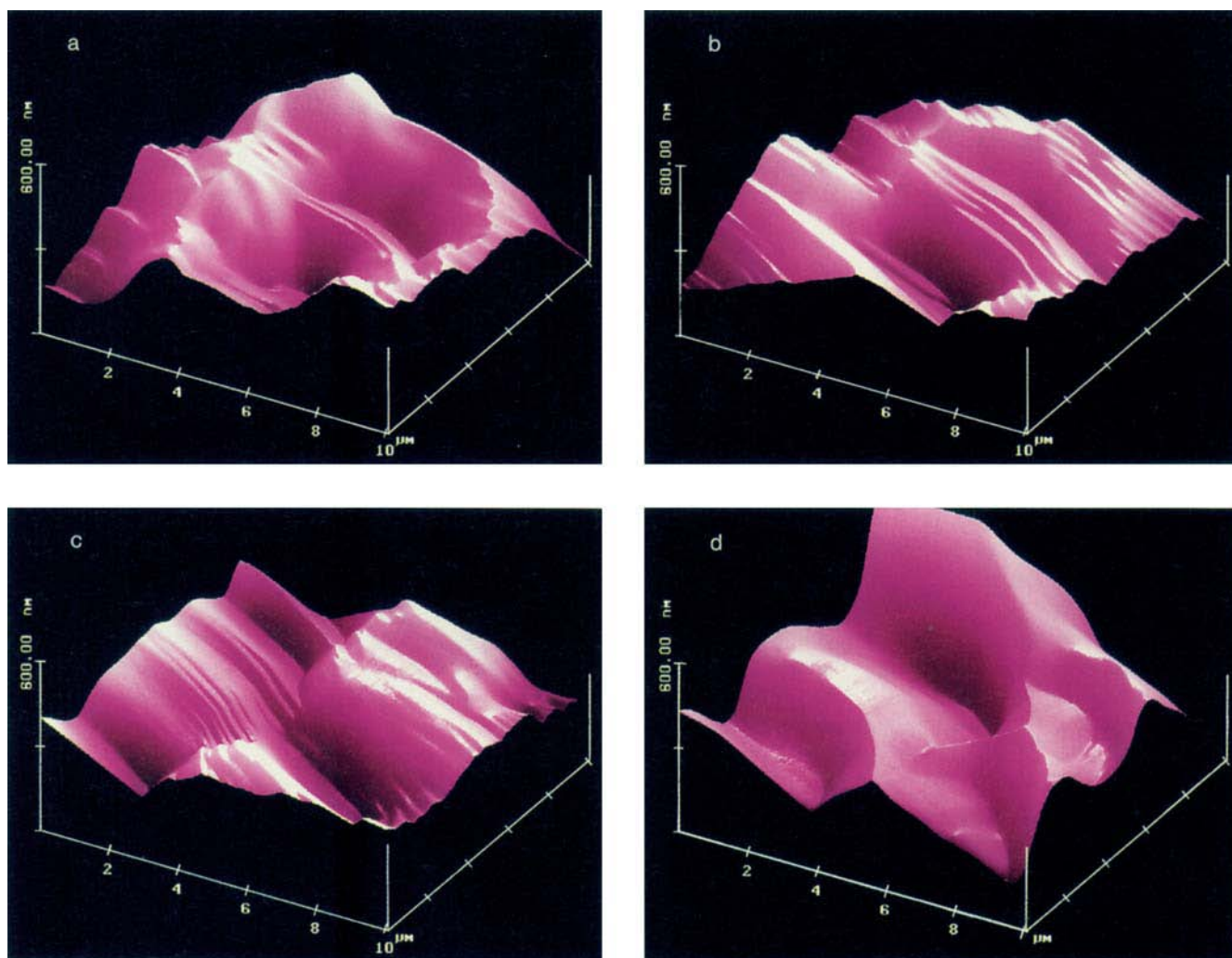


Figure 7. AFM surfaces of **18** (sublimed) on (001); a: fresh after some manipulation in laboratory air; b: after 2 min, c: after 4 min, d: after 6 min of exposure to acetone vapor

the various stages of the reaction remains to be elucidated^[15]. However, a look at the space-filling molecular packing of **18**^[17] (Figure 8) shows that, indeed, there will be a tendency to create edges along [010], the direction in which the original molecules **18** are most densely packed in interlocked rows. Molecular transports must profit from the free space between the rows. Thus, the previous theory^[17] needs some revision in the light of the AFM evidence.

Our new imbibitions are a considerable extension to the previously known systems^[16a,17]. They add remarkable features which make them interesting for applications: Further gases or vapors can be imbibed from the gas phase^[13]. This finding opens the possibility of inclusion of several contaminants at the same time, if those can coexist within the same host lattice. Furthermore, separations of gases may be achieved if some of them are not imbibed at all from the gas phase to a particular host whereas others are. Coexistence of acetone (**2**) occurs quite unexpectedly with *tert*-butyl methyl ether (TBM), tetrahydrofuran (THF), and dioxan in **19** and **18**. From 1:1:1:1 mixtures these hosts imbibe **2**, TBM, THF, and dioxan in the molar ratios of

1.4:1.4:1.0:0.2 and 1:3:4:2. Thus, in the case of **19** acetone (**2**) and TBM are preferred guests, whereas **18** prefers THF and TBM. Such coexistences have not been described for inclusion by crystallization. The new findings allow separations of imbibable gases from nonimbibable ones and this may be of interest for gas purification. Thus, **17** and **20** do not imbibe hexane or cyclohexane (whereas **18** does). Also, **20** does not imbibe THF. On the other hand, **16** does imbibe THF (also benzene, toluene, and ethanol) from the gas phase. Therefore, despite the above coexistences, **2** may be separated from any of these gases by gas-phase imbibition techniques^[22]. This approach has been reviewed for many volatile liquids recently^[13].

Conclusions

Gas/solid reactions with acetone are very efficient and clean. They save resources and avoid wastes in organic syntheses of widely used products. The AFM measurements show beyond doubt that all of the known examples start from the surface. Very distinct features and the differences on very flat or rough portions on (100) of *rac*-**10** prove that

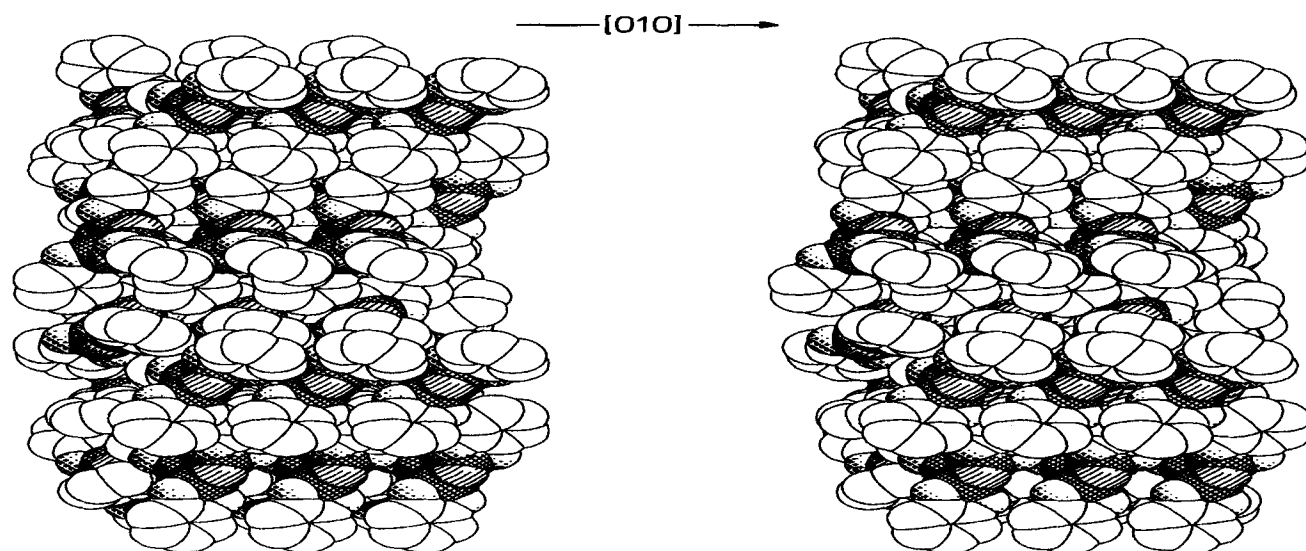


Figure 8. Stereoscopic view of the molecular packing of guest-free monoclinic phosphazene **18** ($P2_1/n$) on (001); P with grid, N with lines, O with dots

the crystal bulk dictates the phase-rebuilding mechanism. Even more striking evidence for this conclusion has been found in related gas/solid reactions where different crystallographic faces can be aligned and scanned with the AFM revealing characteristically different features on the different faces^[3,4]. Nonreactivity has been found if no reasonable phase-rebuilding mechanism is available to the crystal and if the surfaces passivate themselves.

Further AFM measurements in comparison with scanning near-field optical microscopy (SNOM) or light (including X-ray) tunneling (for a recent review see the references cited in ref.^[1,5]), which will be commercially available in the near future, will be necessary to obtain a still more profound understanding of gas/solid reactivity and to identify chemical structures/compositions within the features. These experiments will be important even if the preparative runs afford the chemically analyzed products in quantitative yield. Up till now 8 basic phase-rebuilding mechanisms have been uncovered and wherever possible correlated with X-ray structures of the starting crystals^[3,4,15]. Thus, there exists a sound basis already in this new field of synthetic research, and we are not far from predicting gas/solid reactivity if the crystal structures are known.

There can be no doubt, that many more carbonyl reactions of volatile aldehydes and ketones will be possible and save resources by avoiding excessive and unnecessary waste. Some further examples have been already reported^[12], and the preparation of aromatic and aliphatic imines (Schiff bases) from solid primary amines or their salts awaits exploration.

This work has been supported by a research grant of the *Bundesminister für Forschung und Technologie (BMFT)*, project No. 01VQ9027. We are indebted to the *Schering AG*, Berlin for cooperation and support, in particular through Dr. *W. Beckmann*, Dr. *T. Bemminghaus*, and Dr. *E. Bresinsky*. *K. Bartsch* is thanked for some inclusion experiments and several TGA measurements.

Experimental

The AFM was a Digital Instruments NanoScope II version in connection with NanoScope III imaging software^[3,4]. Si_3N_4 standard tips (vertex angle 45°) on symmetric cantilevers (spring constant 0.12 Nm^{-1}) were chosen under the microscope at 400-fold magnification^[3,4]. They were non-abrasive^[4b]. The NanoScope II was run with head D, the forces were set at 10–30 nN throughout in constant height mode in ambient atmosphere, and 6–10- μ scans were routinely recorded at 3.55 and 4.73 Hz (400×400 points). Changes within that range were not critical but were initially optimized together with the scan angle ($0\text{--}360^\circ$) for best appearance of the final pictures and then kept constant for the reaction sequence under consideration^[3,4]. This implies that all features looked alike at view angles of 0° , 90° , 180° , 270° . Stability of the images was checked for at least 10 scans^[3,4], absence of frictional wear was continuously checked as described in detail elsewhere^[3b,4b]. Nanoliquids have been excluded according to the procedures described in ref.^[1,3b]. There was no trouble of finding the previous surface area within better than 300 nm on reengagement after interruption of the scanning for several hours, provided the sample had not been removed from the AFM stage^[3,4]. Single crystals were mounted as flatly as possible on the scanner by means of a magnetic plate and a sticky black tab (Plano) with the desired face on top. Ambient acetone vapor was generated under the AFM stage by placing a piece of filter paper close to the sample and putting 5 drops of **2** on it. The paper was replaced during scans. Image processing was done by mixing illumination and color coding for height for best appearance. Planefit was used throughout, median and low-pass filtering only sparingly and without loss of information if the glossiness of the pictures could be improved^[3,4]. Packing diagrams were constructed at an IBM RS 6000 AIX-UNIX workstation by using SCHAKAL 93 from *E. Keller*, Freiburg. Single crystals were prepared by slow evaporation of concentrated solutions in the indicated solvents. Compound **18** was sublimed three times at 200°C in vacuo. Differential scanning calorimetry (DSC) was performed with a DSC model 7, thermogravimetric analysis (TGA) with a TGA 7, FT-IR spectra (KBr) with a model 1720, GLC with a GC 8420, all from Perkin-Elmer. The inflection point of the TGA desorption curve ($20^\circ\text{C min}^{-1}$) was taken as the desorption temperature. True density and specific sur-

face measurements were carried out with a DENARMAT equipped with a krypton sensor of Stroehlein Ltd. The two-point BET technique was applied for the calculation. Melting points, specific rotations, and common spectroscopic data of known compounds corresponded within reasonable limits with data from the literature.

o-Phenylenediamine Dihydrohalides (**1** · 2 HX): Typically, crystalline **1a** or **1d**, 30 g (0.28 or 0.20 mol), was placed in a 3-l flask which was evacuated and rotated with a rotatory evaporator, which was connected to an HCl cylinder fitted with a high-grade steel manometer. HCl gas was slowly introduced up to a pressure of 0.5 bar. The reaction started immediately with heat evolution. The rotating flask was immersed in an ice bath, and the pressure maintained at about 0.5 bar by feeding in further HCl gas by using the control of the needle valve at the cylinder. After 1 h, when the gas uptake became slower, the ice bath was removed, the pressure increased to 1 bar and the closed system left for ca. 12 h for completion of the reaction (a refill may be necessary if the available volume was not large enough). The microcrystalline powder **1a** · 2 HCl (50 g, 100%) or **1d** · 2 HCl (46 g, 100%) was analyzed by the weight increase, acid/base titration (phenolphthaleine), m.p. (Table 1), and spectroscopy.

Reaction of Acetone Vapor with Solid o-Phenylenediamine Salts (**1** · 2 HX), *Solid 2-Aminothiophenol* (**6**), *D*-**8** · HCl, *DL*-Penicillamine Hydrochloride (**10** · HCl), and *L*-Cysteine Hydrochloride (**12** · HCl): 80 mmol of **1** · 2 HX (around 20 g) were placed in a 10-l desiccator, evacuated and connected to a 100-ml flask containing 160 to 200 mmol (9.3 to 11.6 g) of acetone which had previously been degassed in vacuo and cooled with liquid nitrogen. Upon removal of the cooling bath the acetone evaporated smoothly. After standing for ca. 12 h, excess gas was condensed back into the flask (77 K). The raw material was titrated with NaOH against phenolphthaleine and characterized by IR, ¹H NMR, and MS/CI. The free bases may be liberated with NaOH in water. The reactions of **1b** · 2 HCl, **1c** · 2 HCl, **6**, *D*-**8** · HCl, *L*-**8** · HCl · H₂O, *DL*-**10** · HCl, and *L*-**12** · HCl were performed on a 1-g scale. Compounds (*R*)-**9** · HCl, (*RS*)-**11** · HCl^[23], and *L*-**13** · HCl^[24] were characterized by their known melting points and optical rotations, the latter after neutralization with NaOH. The reaction of **1d** · 2 HCl in 500 ml of acetone (boiling and standing for several days) yielded **4d** (Table 1).

3a^[7a]: ¹H NMR (D₂O): δ = 7.7–7.6 (1H), 7.2–7.1 (1H), 7.0–6.9 (2H), 2.80 (s, 3H), 2.45 (s, 2H), 1.40 (s, 6H). – ¹³C NMR (CDCl₃): δ = 172.26, 140.70, 137.89, 126.83, 125.45, 122.00, 121.68, 68.25, 45.09, 30.44 (2C), 29.80. – IR (KBr): ν̄ = 1632 cm⁻¹ (C=N). – MS/CI (Isobutane): *m/z* = 189 [M⁺+1].

3b: ¹H NMR ([D₆]DMSO): δ = 7.1–7.0 (1H), 6.8–6.7 (1H), 6.75–6.65 (1H), 2.8 (s, 3H), 2.22 (s, 3H), 2.18 (s, 2H), 1.3 (s, 6H).

3c: ¹H NMR (CDCl₃): δ = 6.93 (s, 1H), 6.52 (s, 1H), 2.80 (br. s, 1H), 2.34 (s, 3H), 2.20 (s, 2H), 2.19 (s, 3H), 2.18 (s, 3H), 1.32 (s, 6H). – ¹³C NMR (CDCl₃): δ = 171.42, 138.49, 135.55, 133.64, 129.94, 127.88, 122.75, 67.78, 45.28, 30.35 (2C), 29.78, 19.17, 18.80. – IR (KBr): ν̄ = 1635 cm⁻¹ (C=N). – MS (70 eV): *m/z* (%) = 216 (24) [M⁺], 201 (100), 162 (29), 161 (35), 146 (18), 91 (7).

3d^[7b]: ¹H NMR ([D₆]DMSO): δ = 8.85–8.75 (1H), 8.1–8.0 (1H), 7.25–7.15 (1H), 3.2 (s, 2H), 2.9 (s, 3H), 1.9 (s, 6H). – ¹³C NMR (CDCl₃/[D₆]DMSO): δ = 170.73, 145.20, 137.97, 132.48, 126.26, 121.26, 118.33, 60.83, 45.69, 30.24, 30.24, 29.91. – IR (KBr): ν̄ = 1644 cm⁻¹ (C=N), 1600, 1549, 1477, 1389, 1310. – MS/CI (Isobutane): *m/z* = 234 [M⁺+1].

4d: ¹H NMR (D₂O): δ = 8.3–8.1 (1H), 7.9–7.7 (1H), 6.95–6.7 (1H), 1.35 (12H). – MS/CI (Isobutane): *m/z* = 234 [M⁺+1].

Acetone Thiosemicarbazone (15g). – *a) Static Technique*: 1.00 g (11 mmol) of thiosemicarbazide (**14g**) was evacuated in a 1-l flask. 0.70 g (12 mmol) of acetone (**2**) was cooled to 77 K and evacuated in a 100-ml flask. After both flasks had been connected to a vacuum line, the acetone was thawed and evaporated. This setup rested at room temperature for ca. 12 h. Excess **2** and the water of the reaction were evaporated or condensed into the smaller flask. The product^[25] (1.44 g, 100%) melted at 175–178°C and was characterized by TLC and suitable spectroscopic methods.

b) Flow Technique: 10 g (0.11 mol) of **14g** was put on glass wool and covered therewith in a heated glass tube at a filling height of 40 cm. A stream of nitrogen or argon which had passed through 19.2 g (0.33 mmol) of liquid **2** was directed through the column from the top in such a way, that all of the acetone had been transported within about 1 h. Traces of water were removed from the solid in vacuo; yield 14.5 g (100%), m.p. 175–176°C.

Acetone 2,4-Dinitrophenylhydrazone (15k)^[11]: 1.0 g (5.1 mmol) of air-dried (with suction) 2,4-dinitrophenylhydrazine (**14k**) was evacuated in a 250-ml flask and connected with a vacuum line to a 100-ml flask which contained 0.58 g (10 mmol) of degassed acetone (**2**) and left for ca. 12 h. Excess **2** and the water of the reaction were removed by evaporation. 1.2 g (100%) of **15k**, m.p. 126°C, was obtained.

Acetone Semicarbazone Hydrochloride (15d · HCl)^[11]: 1.00 g (9.0 mmol) of semicarbazide hydrochloride (**14d** · HCl) was evacuated in a 1-l flask which was connected with a vacuum line to a 100-ml flask containing 1.57 g (27 mmol) of degassed acetone (**2**). After standing for ca. 12 h, excess gas and the water of the reaction were evaporated or condensed into the smaller flask; yield 1.52 g (100%) of **15d** · HCl, m.p. 148–150°C; HCl content (determined acidimetrically): calcd. 24.1%; found 23.7%.

Acetone 3-Methylbenzothiazol-2(3H)-one Azine (15l)^[26]: 1.00 g (0.56 mmol) of 3-methylbenzothiazol-2(3H)-one hydrazone (**14l**) and 0.97 g (1.68 mmol) of acetone (**2**) were allowed to react as above for 2 d at room temperature. After evacuation, 1.20 g (98%) of **15l**, m.p. 120–122°C, was obtained. ¹H NMR (300 MHz, CDCl₃): δ = 7.39–7.31 (1H), 7.27–7.13 (1H), 7.04–6.88 (2H), 3.52 (s, 3H), 2.11 (s, 3H), 2.06 (s, 3H). – Similarly, (melting points of the products **15** given in parentheses) prehydrated **14b** (deliquescence), prehydrated **14c** (deliquescence), **14e**^[27] (158°C), **14f**^[27] (186°C), **14h**^[11] (140–143°C), **14i** (100–102°C), and **14j**^[11] (134–136°C) were allowed to react. In all cases the condensation products **15** (· HX) were obtained quantitatively [bis(hydrazones) in the cases **14e** and **14f**]. All imino salts could be transformed into their free bases by treatment with NaOH in water.

Surface Hydrates of Hydroxylamine Hydrochloride (14a · HCl) and Hydroxylaminium Sulfate (14b · H₂SO₄): Freshly prepared single crystals of the salts **14a** · HCl or **14b** · H₂SO₄ from methanol were mounted on the AFM stage with their morphologically dominant faces on top and scanned as rapidly as possible in ambient moist air at 18°C. AFM measurements were repeated at appropriate time intervals to detect the buildup of the features. Some “snapshots” are shown in Figures 5a–c and Figures 4a–c. The following control experiments were performed to prove surface hydration: fresh single crystals of the salts **14a** · HCl or **14b** · H₂SO₄ were placed on a sticky black tab (Plano) on a magnetic plate (for quick mounting to the scanner) and evacuated in a 50 ml flask which was connected through a vacuum line with an evacuated 50-ml flask containing 10 ml of water. After 5 h, AFM measurements of the crystal surfaces showed features similar in shape and size to the ones of Figures 5c and 4c. In a similar experiment fresh crystals were evacuated and exposed to 1 bar of dry CO₂ from a steel cylin-

der. After 85 h, AFM measurements showed unaffected surfaces which behaved in moist air under the AFM like the ones shown in Figures 5 and 4. In final control experiments the salts were probed with the AFM in a "liquid cell" which was closed after flushing with dry N₂. No change of the almost featureless surfaces could be detected within 1 h and after 12 h.

Preconditioning (Surface Hydration) of Hydroxylaminium Salts: Commercial salts **14a** · HCl, **14b** · H₂SO₄, and **14c** · H₃PO₄ (Aldrich) of hydroxylamine were left in ambient air over 2 d while being spread in thin layers on filter paper.

Acetone Oxime Hydrochloride (15a · HCl)^[11]: 1.00 g (14.4 mmol) of prehydrated hydroxylamine hydrochloride (**14a** · HCl) and 1.67 g (28.8 mmol) of acetone (**2**) were allowed to react as above for ca. 12 h at room temperature. The partially liquefied reaction product lost its water and solidified upon evaporation; yield 1.58 g (100%) of **15a** · HCl, m.p. 95–97°C; HCl content (determined acidimetrically): calcd. 33.3%; found 32.9%.

Large-Scale Preparation of Acetone Oxime (15c) from Very Diluted Acetone Vapor: Two heatable glass tubes (*l* = 50 cm, i.d. = 20 mm) fitted with glass frits were each loaded with 53.1 g (269 mmol) of ground (0.14 m² g⁻¹) hydroxylaminium phosphate (**14c** · H₃PO₄) and 51.9 g (269 mmol) of purposely not ground (0.10 m² g⁻¹) K₂HPO₄ · H₂O. Both tubes were externally heated to 80°C. Then N₂ or air (1000 ml min⁻¹) was passed through 46.9 g (807 mmol) of acetone (**2**) and then over the solids from the top of the tubes. All of the acetone had reacted within 10 h (78 g m⁻³). Behind the second column were mounted a condenser flask at 0°C in an ice bath and a filter of activated carbon (5 g) to catch the last traces of **15c** which escaped condensation. The product and the water of reaction or crystal water were continuously expelled from the columns and condensed. Only after >75% conversion acetone escaped from the first column (test by VPC) and the second column started to react (at <50 g m⁻³ acetone load its escape from the first column started at >90% conversion). At this stage column 1 had reacted to 94% and column 2 to 6% after consumption of the acetone applied. The condensate consisted of 18.5 g (96%) of water and 58.7 g (99.3%) of crystalline acetone oxime (**15c**). The residual 400 mg (0.7%) of noncondensed **15c** was efficiently and completely adsorbed by 3 g of activated carbon (645 m² g⁻¹) at the exhaust. The reaction may be continued by timely removal of the first column and addition of a fresh third one etc. Thus, the experiment simulated an exhaust gas purification down to zero emission. The reacted column (contracted by less than 10%) contained pure crystalline KH₂PO₄ free of water in analytically pure form. The acetone oxime was separated from water by continuous azeotropic removal with the aid of *tert*-butyl methyl ether (TBM), yielding 18.5 ml of water containing 15 mg of **15c**. The water could also be included into zeolites by passing the gas through a column of molecular sieves (3-Å type) at 80°C (useful capacity 15 weight-%) prior to the condensation of pure crystalline **15c**, m.p. 62–63°C).

Clathrate Formation by Imbibition from the Gas Phase. – *a) Static Technique:* 2 mmol of the ground host was evacuated in a 250-ml flask. This flask and a second evacuated 250-ml flask containing **2** (3 in the case of **20** or 6 in the case of **17**) mmol of acetone (**2**) were connected to a vacuum line. Gas mixtures were applied equimolecularly in a 2-l flask which was connected to a vacuum line after thawing and complete vaporization of **2**. After 1 h, excess gas was condensed into flask 2 and the inclusion product evacuated for 1 h at 5 · 10⁻⁴ Torr.

b) Dynamic Technique: 4.0 mmol of the solid host was packed on glass wool in a column of about 20 cm filling height. A two-necked flask at the bottom contained 230 mg (4.0 mmol) of **2**. A

stream of air (alternatively N₂) was passed at a rate of 60 ml min⁻¹ through the liquid so that it took about 2 h to take all of the acetone with it. For the escape-point detections the amount of **2** needed for complete saturation was applied and the exiting gas condensed in a 77-K trap.

c) TGA Technique: The imbibition of **2** (and other gases) was also studied directly during the TGA while using its MULTIRAMP program in the isothermal mode and a gas selector accessory. The sample purge gas N₂, which had passed through acetone (**2**), was set between 0.14 and 0.25 bar, the balance purge gas between 0.28 and 0.42 bar. These were mixed before meeting the sample. The final weights were obtained in less than 10 min for **18** and less than 30 min for **19**. – Desorption curves/temperatures were determined by TGA at a scanning rate of 20°C min⁻¹ (ambient). For desorption at 10 mbar a membrane pump and control by a needle valve were applied. – Preparative desorptions were achieved by heating to 120°C in vacuo and condensing the liberated gases into a 77-K trap. The gases were analyzed by GC.

- [1] G. Kaupp, D. Matthies, *Mol. Cryst. Liq. Cryst. Inc. Nonlin. Opt.* **1988**, *161*, 119–143; *Chem. Ber.* **1987**, *120*, 1897–1903; **1986**, *119*, 2387–2392; G. Kaupp, C. Seep, *Angew. Chem.* **1988**, *100*, 1568–1569; *Angew. Chem. Int. Ed. Engl.* **1988**, *27*, 1511–1512; G. Kaupp, D. Lübber, O. Sauerland, *Phosphorus Sulfur Silicon* **1990**, *53*, 109–120; G. Kaupp, A. Ulrich, G. Sauer, *J. Prakt. Chem./Chem.-Ztg.* **1992**, *334*, 383–390.
- [2] G. Kaupp, *Mol. Cryst. Liq. Cryst.* **1992**, *211*, 1–15.
- [3] [3a] G. Kaupp, J. Schmeyers, *Angew. Chem.* **1993**, *104*, 1656–1658; *Angew. Chem. Int. Ed. Engl.* **1993**, *32*, 1587–1589. – [3b] G. Kaupp, *Mol. Cryst. Liq. Cryst.* **1994**, *242*, 153–169; *J. Vac. Sci. Technol. B* **1994**, *12*, 1952–1956.
- [4] [4a] G. Kaupp, *GIT Fachz. Labor.* **1993**, *37*, 284–294; 581–586; *Angew. Chem.* **1992**, *104*, 606–609; 609–612; *Angew. Chem. Int. Ed. Engl.* **1992**, *31*, 592–595; 595–598. – [4b] G. Kaupp, M. Plagmann, *J. Photochem. Photobiol., A* **1994**, *80*, 339–407.
- [5] R. Kuhn, F. Zumstein, *Chem. Ber.* **1926**, *59*, 498–498.
- [6] W. Jehn, R. Radeaglia, *J. Prakt. Chem.* **1975**, *317*, 1035–1039.
- [7] [7a] N. Kalyanam, S. G. Majunatha, *Heterocycles* **1991**, *32*, 1131–1136; better yields (77%): W. Ried, P. Stahlhofen, *Chem. Ber.* **1957**, *90*, 815–824. – [7b] Further derivatives: L. K. Mushalko, V. A. Chuiguk, *Ukr. Khim. Zh.* **1969**, *35*, 740–746; *Chem. Abstr.* **1969**, *71*, 125957 g.
- [8] **7** has been prepared from **6** in liquid acetone: H. J. Teuber, H. Waider, *Chem. Ber.* **1958**, *91*, 2341–2344.
- [9] H. E. Howard-Lock, C. J. L. Lock, P. S. Smalley, *J. Crystallogr. Spectrosc. Res.* **1983**, *13*, 333–353; the crystal structures of the pure enantiomers and of the unhydrated hydrochlorides are not known; however, the hydrate 1-**8** · HCl · H₂O has been investigated: S. N. Rao, R. Parthasarathy, F. E. Cole, *Acta Crystallogr., Sect. B: Struct. Crystallogr. Cryst. Chem.* **1973**, *B29*, 2373–2378.
- [10] G. Kaupp, D. Matthies, C. de Vrese, *Chem.-Ztg.* **1989**, *113*, 219–220.
- [11] Z. Rappoport, *CRC Handbook of Tables for Organic Compound Identifications*, 3rd ed. CRC Press, Boca Raton, Florida, **1967**.
- [12] G. Kaupp (University of Oldenburg), *German Offen.* DE 4129757, **1993**; *Chem. Abstr.* **1993**, *119*, 138740y.
- [13] G. Kaupp, U. Pogodda, K. Bartsch, J. Schmeyers, A. Ulrich, E. Reents, M. Juniel, *Minderung Organischer Luftschadstoffemissionen mittels Gas-/Festkörper-Reaktionen, Bericht des Bundesministers für Forschung und Technologie*, No. 01VQ9027, 31. 3. **1993**; available from Technische Informationsbibliothek D-30167 Hannover, Welfengarten 1B, Germany.
- [14] See e.g. *Gmelin Handbook System No. 23, NH₃*, **1936**, p. 589 with various references.
- [15] It is not clear yet if AFM measurements^[3,4] will be able to answer that question by comparing initial phase-rebuilding features with the surface structure of recrystallized specimens in the submicroscopic range. However, scanning near-field optical microscopy (SNOM) and X-ray tunneling will certainly be very helpful; for a review of these prospects see: G. Kaupp, *Adv. Photochem.* **1994**, *19*, 119–177.
- [16] [16a] L. J. Barbour, M. R. Cairns, L. R. Nassimbeni, *J. Chem. Soc., Perkin Trans. 2* **1993**, 2321–2322; D. R. Bond, L. John-

- son, L. R. Nassimbeni, F. Toda, *J. Solid State Chem.* **1991**, *92*, 68–79. – ^[16b] E. Weber, M. Czugler, *Top. Curr. Chem.* **1988**, *149*, 45–135; there further acetone clathrates.
- ^[17] ^[17a] H. R. Allcock, M. L. Levin, R. R. Whittle, *Inorg. Chem.* **1986**, *25*, 41–47. – ^[17b] A similar spontaneous behavior was reported for potassium benzenesulfonate: R. M. Barrer, J. Drake, T. V. Whittam, *Proc. R. Soc. London, A* **1953**, *219*, 32–53. – ^[17c] More recent sorptions: E. Weber, C. Wimmer, A. Llamas-Saiz, C. Foces-Foces, *J. Chem. Soc., Chem. Commun.* **1992**, 733–735.
- ^[18] F. Toda, *Top. Curr. Chem.* **1987**, *140*, 43–69.
- ^[19] H. R. Allcock, *J. Am. Chem. Soc.* **1964**, *86*, 2591–2595; H. R. Allcock, L. A. Siegel, *ibid.* **1964**, *86*, 5140–5144.
- ^[20] J. von Braun, *Justus Liebigs Ann. Chem.* **1929**, *472*, 1–89.
- ^[21] I. Goldberg, L. T. W. Lin, H. Hart, *J. Incl. Phenom.* **1984**, *2*, 377–389; H. Hart, L. T. W. Lin, D. L. Ward, *J. Chem. Soc., Chem. Commun.* **1985**, 293–294.
- ^[22] For imbibition from solutions see Highlight by: G. Kaupp, *Angew. Chem.* **1994**, *105*, 768–770; *Angew. Chem. Int. Ed. Engl.* **1994**, *33*, 728–729.
- ^[23] F. P. Doyle, D. O. Holland, P. Mamalis, A. Norman, *J. Chem. Soc.* **1958**, 4605–4614.
- ^[24] F. Micheel, H. Emde, *Chem. Ber.* **1939**, *72*, 1724–1730.
- ^[25] S. Sunner, *Acta Chem. Scand.* **1957**, *11*, 1766–1770.
- ^[26] A. P. D’Rozario, B. Parton, A. Williams, *Gazz. Chim. Ital.* **1987**, *117*, 395–400.
- ^[27] A. C. Brown, E. C. Pickering, F. J. Wilson, *J. Chem. Soc.* **1927**, 107–112; H. W. Stephen, F. J. Wilson, *ibid.* **1926**, 2531–2538. [164/93]